



Published in final edited form as:

*J Am Chem Soc.* 2007 August 8; 129(31): 9789–9798. doi:10.1021/ja072196+.

## Kinetic Isotope Effects for Alkaline Phosphatase Reactions: Implications for the Role of Active Site Metal Ions in Catalysis

Jesse G. Zalatan<sup>†</sup>, Irina Catrina<sup>‡,§</sup>, Rebecca Mitchell<sup>‡</sup>, Piotr K. Grzyska<sup>‡,||</sup>, Patrick J. O'Brien<sup>⊥,#</sup>, Daniel Herschlag<sup>\*,⊥,†</sup>, and Alvan C. Hengge<sup>\*,‡</sup>

Departments of Chemistry and Biochemistry, Stanford University, Stanford, California 94305, Department of Chemistry and Biochemistry, Utah State University, Logan, Utah 84322

### Abstract

Enzyme-catalyzed phosphoryl transfer reactions have frequently been suggested to proceed through transition states that are altered from their solution counterparts, with the alterations presumably arising from interactions with active site functional groups. In particular, the phosphate monoester hydrolysis reaction catalyzed by *Escherichia coli* alkaline phosphatase (AP) has been the subject of intensive scrutiny. Recent linear free energy relationship (LFER) studies suggest that AP catalyzes phosphate monoester hydrolysis through a loose transition state, similar to that in solution. To gain further insight into the nature of the transition state and active site interactions, we have determined kinetic isotope effects (KIEs) for AP-catalyzed hydrolysis reactions with several phosphate monoester substrates. The LFER and KIE data together provide a consistent picture for the nature of the transition state for AP-catalyzed phosphate monoester hydrolysis and support previous models suggesting that the enzymatic transition state is similar to that in solution. Moreover, the KIE data provides unique information regarding specific interactions between the transition state and the active site Zn<sup>2+</sup> ions. These results provide strong support for a model in which electrostatic interactions between the bimetallo Zn<sup>2+</sup> site and a nonbridging phosphate ester oxygen atom make a significant contribution to the large rate enhancement observed for AP-catalyzed phosphate monoester hydrolysis.

### Introduction

Phosphoryl transfer reactions play a fundamental role in a wide range of biological processes including basic metabolism, energy transduction, gene expression, and cell signaling. Uncatalyzed phosphoryl transfer reactions are extremely slow, but enzymes can provide rate enhancements of >10<sup>20</sup>-fold to allow these reactions to occur on a biologically-relevant timescale.<sup>1</sup> As enzymatic rate enhancements can be considered to arise from preferential stabilization of the transition state relative to the ground state,<sup>2–6</sup> characterizing the structure of the transition state is a critical step towards understanding how enzymes interact with and stabilize the transition state to provide the enormous rate enhancements typically associated with biological catalysis.

\*To whom correspondence should be addressed: herschla@stanford.edu, hengge@cc.usu.edu.

<sup>†</sup>Department of Chemistry, Stanford University

<sup>‡</sup>Department of Chemistry and Biochemistry, Utah State University

<sup>§</sup>Present Address: Department of Biological Sciences, Hunter College

<sup>||</sup>Present Address: Department of Microbiology and Molecular Genetics, Michigan State University

<sup>⊥</sup>Department of Biochemistry, Stanford University

<sup>#</sup>Present Address: Department of Biological Chemistry, University of Michigan

**Supporting Information Available:** pH-rate profile for the reaction of mNBP with R166S AP and comparisons with previous data for AP-catalyzed reactions of pNPP and ethyl phosphate. This material is available free of charge via the Internet at <http://pubs.acs.org>.

*Escherichia coli* alkaline phosphatase (AP) is an ideal enzyme for detailed structure-function analysis directed at understanding the nature of the enzymatic transition state. The AP active site contains two Zn<sup>2+</sup> ions and an arginine residue that are positioned to interact with the substrate, and a serine alkoxide that displaces the leaving group in the first step of the reaction to produce a covalent enzyme-phosphate intermediate (Scheme 1).<sup>7-9</sup> This intermediate is hydrolyzed in the second step of the reaction.<sup>9</sup> Of particular importance for mechanistic analysis is AP's relatively low substrate specificity, which has allowed linear free energy relationship (LFER) studies to be performed. These studies have suggested that the transition state for AP-catalyzed phosphate monoester hydrolysis is loose, similar to that in solution.<sup>10-13</sup> The results obtained with AP are consistent with an emerging body of experimental data in a few well-studied enzyme systems suggesting that the transition states for enzyme catalyzed phosphoryl transfer reactions are similar to those in solution.<sup>14</sup>

Suggestions that enzymes alter the nature of the transition state for phosphoryl transfer reactions remain widespread,<sup>15</sup> despite the increasing number of experimental studies suggesting otherwise. Thus, we sought to further test the conclusions of the LFER analysis by measuring kinetic isotope effects (KIEs) for AP-catalyzed reactions with several substrates. KIEs report on the nature of the transition state as well as interactions between the transition state and enzyme functional groups and provide information complementary to that obtained from LFER studies.<sup>16</sup> The KIE approach involves the smallest possible perturbation to a specific site in the substrate, and thus circumvents many of the limitations of site-directed mutagenesis in providing information about specific active site interactions.<sup>17</sup>

The results described herein are consistent with the conclusion from LFER studies suggesting that the transition state for AP-catalyzed phosphate monoester hydrolysis is loose, similar to that in solution. The KIE data further provide strong evidence in support of a model in which electrostatic interactions between the bimetallo Zn<sup>2+</sup> site and a nonbridging phosphate ester oxygen atom make a significant contribution to the large rate enhancement observed for AP-catalyzed phosphate monoester hydrolysis.

## Methods

### Materials

The plasmids for expression of wt and R166S AP and the *phoA*<sup>-</sup> strain of *E. coli* (SM547) were provided by Evan Kantrowitz.<sup>18</sup> Natural abundance and isotopically labeled *p*-nitrophenyl phosphate (pNPP), *p*-nitrophenyl phosphorothioate (pNPPS), and *m*-nitrobenzyl phosphate (mNBP) were synthesized as previously described.<sup>19-21</sup> All other reagents were obtained from commercial sources.

### Purification of Wild Type and R166S AP

Wild type and R166S AP were purified as previously described,<sup>22</sup> except that the dialysis step was omitted. Protein concentration was determined by absorbance at 280 nm using a calculated extinction coefficient of  $3.14 \times 10^4 \text{ M}^{-1} \text{ cm}^{-1}$  (in monomer units).<sup>23</sup>

### AP-catalyzed mNBP Hydrolysis

Reactions were performed with 0.1 M NaMOPS, pH 8.0, 0.5 M NaCl, 1 mM MgCl<sub>2</sub>, and 0.1 mM ZnSO<sub>4</sub> at 25 °C. Reactions were monitored using a malachite green assay to detect release of inorganic phosphate. Malachite green solutions were prepared and inorganic phosphate was assayed as previously described,<sup>24</sup> except that Triton X-100 was used in place of Sterox. Appearance of inorganic phosphate was monitored by removing 100 μl aliquots from the enzymatic reaction and quenching in 800 μl of the malachite green

solution, which contains strong acid. After 1 minute, 100  $\mu\text{l}$  of a 34% sodium citrate solution was added. After 30 minutes, absorbance at 644 nm was measured in a Uvikon 9310 spectrophotometer. Rate constants for R166S AP-catalyzed pNPP hydrolysis obtained from the malachite green assay agreed within 10% with those obtained by continuously monitoring release of *p*-nitrophenolate at 400 nm.

Reactions of mNBP were typically followed to completion ( $\geq 10$  half lives). Rate constants were obtained by nonlinear least-squares fits to a single exponential to yield  $k_{\text{obs}}$ , which is the product of the enzyme concentration and the apparent second-order rate constant  $k_{\text{cat}}/K_{\text{M}}$  under the subsaturating reaction conditions used herein. Reactions were shown to be first order in substrate and enzyme by varying their concentrations over at least a 10-fold range. To ensure that reactions of wt AP were conducted under  $k_{\text{cat}}/K_{\text{M}}$  conditions, these reactions were conducted in the presence of 1 mM sodium tungstate, an inhibitor of AP.<sup>12</sup> The value of  $k_{\text{cat}}/K_{\text{M}}$  could then be calculated from the observed second order rate constant with inhibition and the known inhibition constant for tungstate ( $K_{\text{I}} = 1.1 \mu\text{M}$  at pH 8.0).<sup>12</sup>

### Isotope Effect Determinations

<sup>18</sup>O KIEs were measured using isotope ratio mass spectrometry by the remote label method, using the nitrogen atom as a reporter for isotopic fractionation at the bridge or nonbridge oxygen atoms. The experimental procedures used to measure these isotope effects were similar to those previously reported.<sup>16</sup>

All kinetic isotope effect experiments were run at least in triplicate. Tests were run to determine enzyme and substrate concentrations to ensure that the enzymatic rates of reaction were at least 50 times faster than the aqueous hydrolysis. Background nonenzymatic hydrolysis was a concern with pNPPS but not with mNBP, since the uncatalyzed hydrolysis of the latter substrate is extremely slow.

Isotope effects were calculated from the isotopic ratios at partial reaction in the product ( $R_{\text{p}}$ ), in the residual substrate ( $R_{\text{s}}$ ), and in the starting material ( $R_{\text{o}}$ ).

$$\text{KIE} = [\log(1 - f)] / \{\log[1 - f(R_{\text{p}}/R_{\text{o}})]\} \quad (1)$$

$$\text{KIE} = [\log(1 - f)] / \{\log[(1 - f)(R_{\text{s}}/R_{\text{o}})]\} \quad (2)$$

Equations 1 or 2 were used to calculate the observed isotope effect either from  $R_{\text{p}}$  and  $R_{\text{o}}$  or from  $R_{\text{s}}$  and  $R_{\text{o}}$ , respectively, at the measured fraction of reaction.<sup>25</sup> The observed isotope effects from experiments to determine <sup>18</sup>O isotope effects were corrected for the <sup>15</sup>N effect and for incomplete levels of isotopic incorporation in the starting material as previously described.<sup>26</sup> The independent calculation of each isotope effect using  $R_{\text{p}}$  and  $R_{\text{o}}$  and using  $R_{\text{s}}$  and  $R_{\text{o}}$  from Eqs. 1 and 2, respectively, provided an internal check of the results.

### KIEs for AP-catalyzed pNPPS Hydrolysis

The reactions catalyzed by wt AP were performed in 10 mL of 0.1 M Tris·HCl, pH 9.0, 1 mM MgCl<sub>2</sub>, 1 mM ZnSO<sub>4</sub>, and 10 mM pNPPS at 35 °C. The reactions catalyzed by R166S AP were performed in a 2.5 mL volume of 0.5 M Tris·HCl, pH 8.0, 100  $\mu\text{M}$  MgCl<sub>2</sub>, 10  $\mu\text{M}$  ZnSO<sub>4</sub>, and 40 mM pNPPS at 25 °C. The enzyme concentration was 1  $\mu\text{M}$ . After partial hydrolysis (ranging from 35 to 65%), the reactions were stopped by lowering the pH to 5.5 through addition of cold 0.2 M glycine buffer (pH 2) and placed on ice. From each reaction mixture, two aliquots were taken; one 50  $\mu\text{L}$  aliquot was added to a cuvette containing 3 mL

of 0.1 N NaOH and the absorbance at 400 nm was used to determine the concentration of *p*-nitrophenol at partial hydrolysis. The second aliquot was adjusted to pH 2 in glycine buffer and allowed to react at 50 °C for 12 hours to completely hydrolyze the remaining substrate. Control experiments showed that 12 hours corresponds to >10 times the half-life for pNPPS hydrolysis under these conditions. Subsequently, a 50  $\mu$ L aliquot of this sample was added to 3 mL of 0.1 N NaOH and the absorbance at 400 nm was used to determine the concentration of *p*-nitrophenol product at complete hydrolysis, which corresponds to the initial concentration of substrate. The concentration of *p*-nitrophenol at partial hydrolysis and the initial concentration of substrate were used to determine the fraction of reaction.

The reaction solutions at pH 5.5 were extracted three times with an equal volume of diethyl ether to quantitatively remove the product of the partial hydrolysis, *p*-nitrophenol. The water layers were titrated to pH 2 and allowed to react overnight at 50° C to completely hydrolyze the residual substrate. The *p*-nitrophenol formed was then extracted using the same procedure as described above. The ether layers were dried over MgSO<sub>4</sub>, filtered, and evaporated until dryness. The *p*-nitrophenol was sublimed under vacuum at 90 °C, and 1–1.5 mg samples were prepared for isotopic analysis using an ANCA-NT combustion system coupled with a Europa 20–20 isotope ratio mass spectrometer.

### KIEs for AP-catalyzed mNBP Hydrolysis

AP-catalyzed mNBP hydrolysis reactions were performed in 5 mL of NaMOPS, pH 8.0, 1 mM MgCl<sub>2</sub>, 100  $\mu$ M ZnSO<sub>4</sub>, and 20 mM mNBP at 30 °C and an enzyme concentration of 0.3  $\mu$ M. <sup>31</sup>P NMR was used to monitor reaction progress. After partial reaction (ranging from 40 to 80%), the reactions were stopped by titration to pH 4. NMR was used to obtain the fraction of reaction from integrations of the signals from substrate and inorganic phosphate. The reaction mixtures were extracted with 25 mL of diethyl ether four times to obtain the *m*-nitrobenzyl alcohol product. The ether layers were dried over MgSO<sub>4</sub>, filtered, and evaporated until dryness. The aqueous layer was titrated to pH 8 and about 1 mg of commercial alkaline phosphatase was added to hydrolyze the remaining substrate. After 12 hours, this mixture was titrated to pH 4 and treated as before to recover the liberated *m*-nitrobenzyl alcohol. The *m*-nitrobenzyl alcohol samples were further purified by distillation under vacuum at ~105 °C onto a cold finger apparatus, and samples were then subjected to isotopic analysis, as described above.

## Results and Discussion

Decades of extensive mechanistic studies have strongly suggested that phosphate monoester hydrolysis in solution proceeds through a loose transition state, with nearly complete bond cleavage to the leaving group and little bond formation to the nucleophile (Scheme 2).<sup>19, 27–31</sup> Results from linear free energy relationship (LFER) experiments suggest that AP-catalyzed phosphate monoester hydrolysis also proceeds through a loose transition state, indistinguishable from that in solution.<sup>10–13, 32</sup> To gain further insight into the nature of the transition state for AP-catalyzed phosphate monoester hydrolysis, we have compared the reactivity of AP with several classes of phosphate ester substrates and determined KIEs for representative members of these classes. The KIEs were determined by the competitive method and are therefore effects on  $V/K$  (i.e.,  $k_{\text{cat}}/K_M$ )<sup>16</sup> that reflect differences between the enzymatic transition state and the ground state in which the enzyme and substrate are free in solution.

In addition to characterizing the nature of the transition state, the KIE data have allowed us to compare AP-catalyzed reactions of alkyl and aryl phosphates. AP catalyzes reactions of alkyl phosphates with significantly greater catalytic proficiency than reactions of aryl phosphates.<sup>33</sup> To probe the origin of this effect, we have obtained KIEs with two phosphate

monoester substrates with significantly different leaving groups: *p*-nitrophenyl phosphate (pNPP) and *m*-nitrobenzyl phosphate (mNBP) (Figure 1). Both of these substrates have nitrogen containing functional groups that allows high precision KIE measurements using the remote-label method.<sup>16</sup> The  $pK_a$  of the *p*-nitrophenyl leaving group of pNPP is 7.1,<sup>34</sup> and this substrate has been routinely used in studies of phosphatase enzymes such as AP.<sup>12</sup> In contrast, mNBP has not previously been studied as a substrate of AP. The high  $pK_a$  of the *m*-nitrobenzyl leaving group of mNBP ( $pK_a = 15$ )<sup>35</sup> is expected to lead to reactivity analogous to that of alkyl phosphates, which have similar leaving group  $pK_a$  values. The *m*-nitrobenzyl leaving group has been used previously in studies of both solution and enzyme-catalyzed phosphoryl transfer reactions and has been particularly valuable in allowing KIE comparisons between alkyl and aryl phosphates.<sup>21, 35–37</sup> We first compare the reactivity of aryl, alkyl, and benzyl phosphates in AP-catalyzed reactions and then analyze the KIE data in the context of these reactivity comparisons. Finally, we consider KIE data for AP-catalyzed *p*-nitrophenyl phosphorothioate (pNPPS) hydrolysis, and the results reinforce the conclusions from the analysis of phosphate monoester substrates.

### Reactivity Comparisons of Nonenzymatic Reactions

Before comparing the reactivity of AP with alkyl, benzyl, and aryl phosphates, it is important to determine whether these compounds react via similar mechanisms in solution. The dianionic forms of the phosphate esters (Scheme 3) are the substrates for AP,<sup>12</sup> but kinetic constants for the corresponding nonenzymatic reactions of alkyl and benzyl phosphate dianions cannot be readily measured, as these reactions are extremely slow and can proceed via C-O bond cleavage instead of P-O cleavage.<sup>1, 38–40</sup> The nonenzymatic reactions of alkyl, aryl, and benzyl phosphate monoanions react via P-O cleavage and rates can be measured, however.

Reactions of phosphate monoester monoanions have been proposed to proceed with proton transfer from the phosphoryl group to the leaving group in the transition state, thereby neutralizing the charge that would otherwise develop on the leaving group oxygen.<sup>19, 21, 28, 38–41</sup> The available literature data for alkyl, aryl, and benzyl phosphate monoanions suggest that each of these classes of compounds react via this mechanism. Hydrolysis reactions of alkyl and aryl phosphate monoanions follow the same leaving group dependence, with little change in the hydrolysis reaction rate with leaving group  $pK_a$ , consistent with the long-standing mechanistic proposal for proton transfer in the transition state.<sup>28, 41</sup> The hydrolysis of benzyl phosphate has a similar rate constant and pH-dependence with that observed for alkyl phosphate hydrolysis, except under strong acid conditions in which the neutral benzyl phosphate reacts via C-O cleavage.<sup>38, 39, 42</sup> Thus, there appears to be no substantial difference in the intrinsic reactivity of alkyl, aryl, and benzyl phosphates, beyond effects from the differential stability of the leaving groups that is reflected in the different  $pK_a$  values.

### Reactivity Comparisons of AP-Catalyzed Reactions

Figure 2 shows a compilation of kinetic data for the reactions of wild type (wt) AP and a mutant of AP with the active site Arg replaced by Ser (R166S AP), represented by closed and open symbols, respectively. R166S AP has been used in a number of mechanistic studies of AP,<sup>10, 32, 43, 44</sup> in part because it is not subject to the severe product inhibition that has often complicated mechanistic studies of wt AP.<sup>12</sup> The different substrate classes and the symbols used to represent them in Figure 2 are depicted in Scheme 3. Rate constants for reactions of mNBP<sup>2-</sup> with wt and R166S AP (circles) were determined in this work, and all other rate constants are from previous work.<sup>10, 12</sup>

The rates of reaction of the alkyl, aryl and benzyl phosphates with AP differ considerably, even after accounting for differential leaving group stability. Reactions of substrates with low  $pK_a$  leaving groups, such as aryl phosphates, with wt AP are limited by binding rather than the chemical step and are independent of leaving group  $pK_a$  (dashed line).<sup>12, 45, 46</sup> Rate constants for alkyl phosphates with good leaving groups such as trifluoroethyl phosphate and propargyl phosphate (leaving group  $pK_a$  values of 12.4 and 13.6, respectively) also fall on the dashed line, suggesting that these reactions may not be limited by the chemical step. In contrast, the rate constants for less reactive alkyl phosphates are smaller and depend on leaving group  $pK_a$ , suggesting that the chemical step is rate-determining. The slope of the line correlating the log of the rate constant with the  $pK_a$  of the leaving group (the Brønsted coefficient,  $\beta_{lg}$ ) is  $-0.85$ .<sup>12</sup> The values of  $\beta_{lg}$  for alkyl phosphates are nearly the same for wt and R166S AP (Figure 2), suggesting that the interaction of the Arg side chain with the nonbridging phosphoryl oxygen atoms does not alter the nature of the transition state.<sup>10</sup> Further, the values of  $\beta_{lg}$  for reactions of aryl phosphorothioate monoesters with both wt and R166S AP are the same and similar to those for the alkyl phosphates.<sup>11, 32</sup> These results are consistent with a similar loose transition state with substantial charge buildup on the leaving group oxygen for reactions of all phosphate monoester substrates, possibly with some lessening of the value of  $\beta_{lg}$  relative to solution reactions due to the electrostatic interaction of the leaving group oxygen atom with an active site  $Zn^{2+}$  ion (see also below).<sup>12, 13</sup>

The enzymatic reactivity of  $mNBP^{2-}$  can be directly compared with that of simple alkyl phosphates, as the leaving groups for these compounds fall in the same  $pK_a$  range. The rate constants for  $mNBP^{2-}$  hydrolysis by wt and R166S AP are  $1.8 \times 10^7$  and  $2.3 \times 10^3 \text{ M}^{-1}\text{s}^{-1}$ , respectively. These values deviate positively from the correlation line for alkyl phosphates for both wt and R166S AP, falling  $\sim 10$ -fold above their expected values (Figure 2; open and closed circles and double-headed arrows). The simplest model for the increased reactivity of  $mNBP^{2-}$  is additional binding interactions with the larger benzyl leaving group (Scheme 3) within the AP active site. In this model, the charge buildup on the bridging oxygen in the transition state for  $mNBP^{2-}$  hydrolysis is likely to be similar to that for simple alkyl phosphates.

An alternative explanation for the enhanced reactivity of  $mNBP$  is a distinct catalytic mechanism involving the monoanion as the substrate for catalysis with intramolecular protonation of the leaving group, although previous studies of both alkyl and aryl phosphates with wt and R166S AP indicate that the dianion is the substrate for catalysis.<sup>12, 22</sup> To examine this possibility, we determined the pH-rate profile for the reaction of  $mNBP$  with R166S AP over the pH range of 7–9. These data were sufficient to confirm that the pH dependence was identical to that observed previously for  $pNPP$  and other phosphate monoester substrates, which react as the dianion,<sup>12, 22</sup> and strongly suggests that  $mNBP$  also reacts as a dianion (Supporting Information). If  $mNBP$  were to react as a monoanion, the pH dependence would have been predicted to deviate substantially from that observed for  $pNPP$ . Thus, there is no indication from the pH-rate profile of a change in rate-limiting step or mechanistic path for the  $mNBP$  reaction from that previously observed for other AP-catalyzed reactions.

In contrast to the positive deviation observed with  $mNBP^{2-}$ , the rate constant for R166S AP-catalyzed  $pNPP^{2-}$  hydrolysis falls  $\sim 10^3$ -fold below the correlation line for the alkyl phosphate rate constants extrapolated to lower  $pK_a$  (Figure 2, dotted line and single-headed arrow). This comparison can only be made for R166S AP, as the reaction of  $pNPP^{2-}$  with wt AP is limited by a non-chemical step (Figure 2, dashed line).<sup>12</sup> Because the leaving group oxygen for  $pNPP^{2-}$  is attached to a secondary carbon whereas the alkyl phosphate leaving groups are primary alkoxides, the deviation could arise from a steric effect. However, rate constants for substrates with *p*-nitrophenyl leaving groups also deviate negatively with

respect to other aryl leaving groups in AP-catalyzed reactions of aryl phosphorothioates,<sup>11, 32</sup> aryl sulfates,<sup>13</sup> methyl phenyl phosphate diesters,<sup>44</sup> and in several solution reactions.<sup>44</sup> This effect presumably arises from greater delocalization of the negative charge into the aromatic ring for *p*-nitrophenolate than for other aryl leaving groups.<sup>44</sup> Thus, the deviation of the rate constant for pNPP<sup>2-</sup> hydrolysis relative to that expected from alkyl phosphate reactions could arise because of differing amounts of negative charge localized on the leaving group oxygen. Alkyl phosphates cannot delocalize charge into an aromatic ring as in aryl phosphates, and are expected to have greater charge localization on the leaving group oxygen in the transition state. Nevertheless, we cannot rule out steric contributions to the deviation observed for pNPP<sup>2-</sup>.

### Kinetic Isotope Effects for AP-catalyzed Reactions

Determination of KIEs for reactions of alkyl and aryl phosphates with AP could provide insight into the nature of the transition state and active site interactions for AP-catalyzed phosphate monoester hydrolysis that is complementary to the information obtained from LFER studies. Because a remote <sup>15</sup>N label is required to achieve the precision needed for these measurements,<sup>16</sup> we used the benzyl phosphate mNBP<sup>2-</sup> (Figure 1), which contains a nitro group that can be used as the remote label. mNBP<sup>2-</sup> has a leaving group p*K*<sub>a</sub> of 15, similar to most alkyl leaving groups and substantially greater than the p*K*<sub>a</sub> of 7 for the aryl leaving group of pNPP<sup>2-</sup>. As noted, above, the electronic properties of the leaving group oxygen for mNBP<sup>2-</sup> are expected to be similar to alkyl phosphates and the KIEs for mNBP<sup>2-</sup> reactions with AP should provide a reasonable model for the behavior of alkyl phosphates in the AP active site.

Heavy atom KIEs were determined at three different positions in each substrate (Figure 1). The <sup>18</sup>O nonbridging effect [<sup>18</sup>(*V/K*)<sub>nonbridge</sub>] is a secondary KIE reporting on changes in both hybridization and bond order. This effect can be diagnostic of the looseness or tightness of the transition state, but can also be perturbed by interactions with the nonbridging oxygen atoms.<sup>16</sup> The <sup>18</sup>O bridging effect [<sup>18</sup>(*V/K*)<sub>bridge</sub>] is a primary KIE that reports on the extent of bond cleavage to the leaving group, and is also sensitive to interactions that stabilize charge buildup such as protonation.<sup>16</sup> Finally, the <sup>15</sup>N label allows <sup>18</sup>O KIE determination by the remote label method. With *p*-nitrophenyl leaving groups, the <sup>15</sup>N effect [<sup>15</sup>(*V/K*)] also reports on charge delocalization into the aromatic ring.<sup>16</sup> No bonding changes at the nitro group are expected during mNBP<sup>2-</sup> hydrolysis, however, and <sup>15</sup>(*V/K*) for mNBP<sup>2-</sup> should be close to unity and can serve as an internal control.<sup>21</sup>

KIEs for AP-catalyzed reactions and corresponding solution reactions are reported in Table 1. KIEs for the reaction of wt AP with pNPP<sup>2-</sup> have been previously reported and are all near unity, consistent with a non-chemical rate-determining step.<sup>19</sup> The KIEs for the reaction of mNBP<sup>2-</sup> with wt AP differ from unity, but are significantly smaller than the KIEs determined for the reaction with R166S AP (see below). The reaction of mNBP<sup>2-</sup> with wt AP is presumably partially limited by a non-chemical step, as the value of *k*<sub>cat</sub>/*K*<sub>M</sub> is close to the limit at which chemistry is no longer rate-determining (Figure 2) and the full isotope effects appear to be masked relative to the isotope effects with a slower, mutant enzyme, R166S AP. Reactions of R166S AP with pNPP<sup>2-</sup> and mNBP<sup>2-</sup> are likely to be limited by the chemical step, as the values for *k*<sub>cat</sub>/*K*<sub>M</sub> are well below the limiting values observed for wt AP (Figure 2). Consistent with this expectation, several of the observed KIEs for these substrates are significantly different from unity (Table 1).

### KIEs for R166S AP-catalyzed pNPP<sup>2-</sup> Hydrolysis

KIEs for the reaction of R166S AP with pNPP<sup>2-</sup> have been previously reported and discussed in the context of reactivity comparisons with *p*-nitrophenyl sulfate.<sup>47</sup> Here we

discuss the implications of the  $\text{pNPP}^{2-}$  reaction KIEs for the nature of the transition state and for comparisons of alkyl and aryl phosphates.

The value of  $^{18}(V/K)_{\text{bridge}}$  KIE for R166S AP-catalyzed  $\text{pNPP}^{2-}$  hydrolysis is 1.0091, significantly reduced from the value of 1.0189 observed for  $\text{pNPP}^{2-}$  hydrolysis in solution (Table 1). Similarly, the value of  $^{15}(V/K)$  of 1.0007 is significantly reduced from its solution value of 1.0028. Both values are closer to those observed for monoanion than dianion hydrolysis in solution, but the  $\text{pNPP}$  dianion is the substrate for AP and no proton transfer to the leaving group in the transition state is expected.<sup>12, 22</sup> One possible interpretation of these results is that the transition state for AP-catalyzed  $\text{pNPP}^{2-}$  hydrolysis is tighter than that in solution, with less bond cleavage to the leaving group. However, previous LFER and KIE data suggest that the transition state for AP-catalyzed phosphate monoester hydrolysis is loose, similar to that in solution.<sup>10–13, 32, 48</sup> Furthermore, if the enzymatic transition state were tighter than that in solution, a normal contribution to the nonbridge KIE would be expected (Figure 3).<sup>16</sup> Instead, the observed value of  $^{18}(V/K)_{\text{nonbridge}}$  for R166S AP-catalyzed  $\text{pNPP}^{2-}$  hydrolysis is 0.9925, significantly more inverse than the solution value of 0.9994 (Table 1). Thus, when taken together the KIEs for R166S AP-catalyzed  $\text{pNPP}^{2-}$  hydrolysis do not suggest a change in the nature of the transition state from that in solution.

We suggest an alternative model in which strong interactions between the substrate and the active site  $\text{Zn}^{2+}$  ions (Scheme 1) result in the observed reductions in the KIEs for R166S AP-catalyzed  $\text{pNPP}^{2-}$  hydrolysis relative to the values for the uncatalyzed reaction. Interactions with the leaving group oxygen atom would be reflected in both  $^{18}(V/K)_{\text{bridge}}$  and  $^{15}(V/K)$ , and interactions with the nonbridging oxygen atom would be reflected in  $^{18}(V/K)_{\text{nonbridge}}$ . The observed inverse contribution to the  $^{18}\text{O}$  isotope effects could arise if coordination to  $\text{Zn}^{2+}$  were to stiffen bending modes or introduce new vibrational modes that involve motions of the substrate oxygen atoms. Coordination of the leaving group oxygen by  $\text{Zn}^{2+}$  would also decrease electron delocalization into the nitro group, leading to the observed decrease in the  $^{15}\text{N}$  isotope effect relative to that in solution (Table 1).

### KIEs for R166S AP-catalyzed $\text{mNBP}^{2-}$ Hydrolysis

Interpretation of the KIEs for enzymatic  $\text{mNBP}^{2-}$  hydrolysis is complicated by the fact that corresponding KIEs for  $\text{mNBP}$  dianion hydrolysis in solution cannot be measured. The observed reaction of  $\text{mNBP}$  in solution is expected to be dominated by reaction of  $\text{mNBP}$  as a monoanion and reaction of the dianion with C-O rather than P-O cleavage.<sup>1, 38–40</sup> In the absence of measured KIEs for the uncatalyzed reaction, reasonable estimates can be made based on available literature data. The value of  $^{18}k_{\text{nonbridge}}$  for  $\text{mNBP}^{2-}$  is likely to be small and inverse, similar to that for  $\text{pNPP}^{2-}$  in solution, because the nonbridging P-O bonds are chemically equivalent in  $\text{mNBP}^{2-}$  and  $\text{pNPP}^{2-}$ . The value of  $^{18}k_{\text{bridge}}$ , however, should be significantly larger for an alkyl leaving group than for an aryl leaving group. The maximum expected  $^{18}\text{O}$  isotope effect for cleavage of a *p*-nitrophenyl leaving group is  $\sim 1.03$ , based on the equilibrium isotope effect for *p*-nitrophenyl acetate hydrolysis.<sup>49</sup> This value is consistent with values of  $^{18}\text{O}$  KIEs of  $\sim 1.02$ – $1.03$  observed for  $\text{pNPP}^{2-}$  hydrolysis under a variety of solution and enzymatic conditions.<sup>16</sup> In contrast to the behavior of aryl leaving groups, departure of a methoxide leaving group in the hydrazinolysis of methyl formate and methyl benzoate gives leaving group  $^{18}\text{O}$  KIEs of 1.06 and 1.04, respectively.<sup>50, 51</sup> Furthermore, C-O cleavage reactions catalyzed by fumarase and crotonase give leaving group  $^{18}\text{O}$  KIEs of 1.07 and 1.05, respectively.<sup>52, 53</sup> Finally, maximum KIE values for C-O and P-O cleavage reactions with alkyl leaving groups of  $\sim 1.05$  have been predicted based on vibrational stretching frequencies.<sup>50, 54</sup> Thus, the value of  $^{18}k_{\text{bridge}}$  for  $\text{mNBP}^{2-}$  hydrolysis in solution proceeding through a loose transition state with nearly complete leaving group bond cleavage is likely to be in the range of  $\sim 1.04$ – $1.06$ , significantly larger than  $^{18}k_{\text{bridge}}$  for nonenzymatic  $\text{pNPP}^{2-}$  hydrolysis.



For R166S AP-catalyzed mNBP<sup>2-</sup> hydrolysis, the value of  $^{18}(V/K)_{\text{bridge}}$  is 1.0199. While this value is larger than the value of 1.0091 observed for R166S AP-catalyzed pNPP<sup>2-</sup> hydrolysis, it represents a significant decrease from the estimated value of ~1.04–1.06 for the mNBP<sup>2-</sup> hydrolysis in solution. As for pNPP<sup>2-</sup>, the reduced value of  $^{18}(V/K)_{\text{bridge}}$  for the enzymatic reaction relative to the solution reaction probably reflects an inverse contribution to the observed KIE from interactions with a Zn<sup>2+</sup> ion in the transition state (Figure 3).

The value of  $^{18}(V/K)_{\text{nonbridge}}$  for R166S AP-catalyzed mNBP<sup>2-</sup> hydrolysis is 0.9933, identical within error to the value of 0.9925 observed for R166S AP-catalyzed pNPP<sup>2-</sup> hydrolysis. This result is consistent with the expectation that the values of  $^{18}k_{\text{nonbridge}}$  for the solution reactions of pNPP<sup>2-</sup> and mNBP<sup>2-</sup> should be similar. Moreover, the value of 0.9933 is significantly more inverse than the expected value in solution and may reflect an inverse contribution to the KIE from interactions with Zn<sup>2+</sup> ions in the transition state, as noted above for the pNPP<sup>2-</sup> reaction (Figure 3).

### The Effect of Metal Ion Coordination on KIEs

The data for AP-catalyzed reactions described herein suggest that coordination to metal ions can lead to stiffening of the vibrational environment of phosphoryl oxygen atoms and an inverse contribution to the observed KIEs.<sup>55</sup> It is well-established that coordination of oxygen to divalent metal ions can give rise to inverse isotope effects both in solution<sup>56, 57</sup> and in enzymatic reactions.<sup>58</sup> Moreover, vibrational spectroscopy studies have demonstrated that metal ion coordination to phosphoryl oxygen atoms can lead to significant perturbations in the frequencies of vibrational modes involving phosphoryl groups.<sup>59–62</sup> This model does not require metal ion coordination to lead to an increase in P-O bond order and a corresponding increase in the frequency of the P-O stretching vibration. Rather, the inverse contribution to the KIE due to metal ion coordination arises from a stiffening of the overall vibrational environment of the phosphoryl oxygen atoms, and this stiffening can involve change in stretching, bending, and torsional vibrational modes.

While literature precedents support the idea that coordination to metal ions in the AP active site leads to inverse contributions to the observed KIEs, such effects may not be a general consequence of metal ion coordination. For example, no significant isotope effect was observed for coordination of Mg<sup>2+</sup> to inorganic phosphate in solution.<sup>63</sup> Suppression of the bridging isotope effect [ $^{18}(V/K)_{\text{bridge}}$ ] due to metal ion interactions has not been previously reported in other systems, although it has been suggested as a possible explanation for the observed bridging KIE for  $\lambda$  protein phosphatase.<sup>64</sup> The available data for the nonbridging KIEs [ $^{18}(V/K)_{\text{nonbridge}}$ ] varies with the system studied. Only small inverse values of  $^{18}(V/K)_{\text{nonbridge}}$  were observed with  $\lambda$  protein phosphatase containing Mn<sup>2+</sup> or Ca<sup>2+</sup> in the active site.<sup>64</sup> However, such studies may not accurately model binding interactions with the bimetallo Zn<sup>2+</sup> cluster in the AP active site. Furthermore, large inverse values of  $^{18}(V/K)_{\text{nonbridge}}$  were observed for the reactions of pNPP<sup>2-</sup> with calcineurin containing Mn<sup>2+</sup> or Mg<sup>2+</sup> in the active site.<sup>65, 66</sup> From the available literature data, it is reasonable to suggest that the inverse contributions to KIEs observed for AP-catalyzed reactions arise from metal ion coordination. Perhaps differences in isotope effects will ultimately aid in distinguishing between different possible transition state coordination geometries in other binuclear metalloenzymes that catalyze phosphoryl transfer reactions.

### KIEs for wt and R166S AP-catalyzed pNPPS<sup>2-</sup> Hydrolysis

We have also determined KIEs for the AP-catalyzed reaction of pNPPS<sup>2-</sup>, an aryl phosphorothioate (Figure 1), and the results reinforce the above conclusions. Phosphorothioate monoesters are analogs of phosphate monoesters with a single sulfur

substitution at a nonbridging position (Scheme 3) and react through similar loose transition states, although bond cleavage to the leaving group may be more advanced.<sup>11, 20, 67</sup> Comparisons of phosphate and phosphorothioate monoesters have previously provided valuable insights into the AP reaction mechanism.<sup>11, 32, 43</sup>

The KIEs for AP-catalyzed pNPPS<sup>2-</sup> hydrolysis are significantly different from unity (Table 1), confirming previous conclusions that the chemical step is rate-determining for phosphorothioate hydrolysis catalyzed by both wt and R166S AP.<sup>11, 32</sup> Furthermore, the KIEs for the wt and R166S AP-catalyzed reactions are identical within error. Indeed, mutation of Arg166 to Ser has no significant effect on  $k_{\text{cat}}/K_M$  for pNPPS<sup>2-</sup> hydrolysis.<sup>68</sup> A similar situation was observed for reactions of AP with phosphate diesters, where reactivity is unaffected by mutation of Arg166 to Ser.<sup>22</sup> Both phosphate diesters and phosphorothioate monoesters have large functional groups (either a second ester group or a sulfur atom) that would result in unfavorable interactions with a positioned active site arginine. The absence of rate effects upon mutation of Arg166 suggests that the arginine side chain can readily move away from the active site to allow diester or phosphorothioate binding and reaction. These data are consistent with pNPPS<sup>2-</sup> binding to the AP active site with a nonbridging oxygen atom coordinated by the two Zn<sup>2+</sup> ions; the alternative in which the sulfur atom coordinates the Zn<sup>2+</sup> ions is discussed below.

The values of  $^{18}(V/K)_{\text{bridge}}$  are 1.0094 and 1.0098 for wt and R166S AP-catalyzed pNPPS<sup>2-</sup> hydrolysis, respectively (Table 1). These values are identical within error to that observed for R166S AP-catalyzed pNPP<sup>2-</sup> hydrolysis, which has the same leaving group, and significantly smaller than the value of 1.0237 for uncatalyzed pNPPS<sup>2-</sup> hydrolysis.<sup>20</sup> As for pNPP<sup>2-</sup> and mNBP<sup>2-</sup>, these data support a model in which coordination of the leaving group oxygen to an active site Zn<sup>2+</sup> suppresses the observed KIE.

The nonbridge  $^{18}\text{O}$  KIE for the uncatalyzed hydrolysis of pNPPS<sup>2-</sup> in solution is 1.0135.<sup>20</sup> This value is significantly larger than the small inverse values typically observed for phosphate monoester hydrolysis (Table 1),<sup>16</sup> even though phosphate monoesters and phosphorothioate monoesters react through similar loose transition states.<sup>11, 20, 67</sup> The large normal value of  $^{18}k_{\text{nonbridge}}$  for pNPPS<sup>2-</sup> has been attributed to a dominant contribution from loosening of bending modes in the transition state for phosphorothioate ester hydrolysis.<sup>20</sup>

The values of  $^{18}(V/K)_{\text{nonbridge}}$  for pNPPS<sup>2-</sup> hydrolysis catalyzed by wt and R166S AP are 0.9760 and 0.9768, respectively (Table 1). As for pNPP<sup>2-</sup> and mNBP<sup>2-</sup>, the enzymatic reaction results in a large inverse contribution to the nonbridging KIEs, consistent with Zn<sup>2+</sup> coordination to a nonbridging oxygen atom restricting bending modes. However, the inverse contribution from AP to  $^{18}(V/K)_{\text{nonbridge}}$  for pNPPS<sup>2-</sup> is far larger than that observed for pNPP<sup>2-</sup> and mNBP<sup>2-</sup>, and suggests that in addition to fixing the position of a nonbridging oxygen atom, the AP active site may more severely constrain bending and torsional vibrations that involve the large sulfur atom of pNPPS<sup>2-</sup>.

An alternative possibility is that pNPPS<sup>2-</sup> binds to the AP site with the sulfur atom coordinated by the two Zn<sup>2+</sup> ions, which would lead to a different interpretation of the observed KIEs. However, the larger size and correspondingly longer bond lengths of sulfur relative to oxygen<sup>69</sup> suggest that sulfur coordination to the active site Zn<sup>2+</sup> ions would require significant rearrangements of the active site, including perturbations of Zn<sup>2+</sup> interactions with the nucleophile and leaving group. If significant rearrangements of the active site coordination environment were to occur, then the values of  $^{18}(V/K)_{\text{bridge}}$  for pNPPS<sup>2-</sup> and pNPP<sup>2-</sup> would be expected to differ, as this KIE reflects interactions of the leaving group with a Zn<sup>2+</sup> ion. Instead, the values of  $^{18}(V/K)_{\text{bridge}}$  for pNPPS<sup>2-</sup> and pNPP<sup>2-</sup>

are the same within error when the chemical step is rate-determining (Table 1). Further, structural studies of Klenow exonuclease, which has a bimetallo active site similar to that of AP, suggest that the metal ions are displaced from the active site upon binding of a phosphorothioate substrate in which the sulfur atom is oriented towards the bimetallo site by remote binding interactions.<sup>70</sup> Thus, it seems likely that pNPPS<sup>2-</sup> binds the AP active site with a nonbridging oxygen atom coordinated by the two Zn<sup>2+</sup> ions.

### Implications for Catalysis

The KIEs observed for AP-catalyzed reactions are consistent with previous conclusions from LFER experiments that the transition state for AP-catalyzed phosphate monoester hydrolysis is loose and similar to that in solution. Furthermore, the KIEs suggest that strong interactions with the active site Zn<sup>2+</sup> ions restrict vibrational motions of the substrate. These interactions occur at the position of bond cleavage, where extensive charge buildup is expected in a loose transition state, and at the nonbridging positions (Figure 3). Previous functional studies have implicated electrostatic interactions between a nonbridging phosphate ester oxygen atom and the active site Zn<sup>2+</sup> ions as being especially important for catalysis,<sup>43, 47</sup> and the KIE data described herein strengthen these conclusions.

AP catalyzes reactions of substrates with poor leaving groups with significantly greater catalytic proficiency than those with good leaving groups.<sup>71</sup> The difference in catalytic proficiency is reflected in the difference between the solution and enzymatic values of  $\beta_{1g}$ , which are -1.23 and -0.85, respectively.<sup>12, 28</sup> This difference corresponds to smaller catalytic proficiencies as the leaving group  $pK_a$  decreases (i.e., for a given decrease in the leaving group  $pK_a$ , the rate of the solution reaction increases more than the rate of the corresponding enzymatic reaction). A significant fraction of the difference in  $\beta_{1g}$  between the solution and enzymatic reaction has been suggested to arise from interactions with an active site Zn<sup>2+</sup> ion.<sup>11-13</sup> I.e., the large difference in catalytic proficiency could arise from competing effects between stabilization of charge buildup by the leaving group itself and stabilization by interaction with the active site Zn<sup>2+</sup>. These stabilizing effects are not simply additive such that a leaving group that is better able to stabilize negative charge buildup would consequently interact more weakly with the active site Zn<sup>2+</sup> than a poor leaving group.

The KIE data for pNPP<sup>2-</sup> and mNBP<sup>2-</sup> suggest that there are strong interactions between the leaving group oxygen and an active site Zn<sup>2+</sup> ion, and it is possible that differences in the strength of this interaction could be responsible for the differing catalytic proficiencies observed for alkyl and aryl substrates. More direct support for this model could be provided if the decrease in the value of  $^{18}(V/K)_{bridge}$  relative to that in solution was larger for mNBP<sup>2-</sup> than for pNPP<sup>2-</sup>. However, this comparison cannot be made due to the absence of experimental KIE data for the mNBP<sup>2-</sup> reaction in solution.

Mechanistic studies of other enzymes support the idea that differences in catalytic proficiency for good and poor leaving groups could arise from differential interactions with active site functional groups. The clearest evidence for this phenomenon has been obtained with glycosyl and phosphoryl transfer enzymes that utilize general acid catalysis.<sup>72-77</sup> For these enzymes, mutation of the residue that acts as the proton donor has a larger deleterious effect for the reactions of substrates with poor leaving groups -i.e., substrates with high  $pK_a$  leaving groups are more greatly impeded by the mutation than substrates with low  $pK_a$  leaving groups. These observations suggest that general acid catalysis makes a larger contribution to catalytic proficiency for substrates with poor leaving groups than for those with good leaving groups, as might be expected based on differential proton affinities.

Enzymes that catalyze phosphoryl transfer reactions are generally observed to have general acids, divalent metal ions, or other charged groups positioned to stabilize negative charge buildup.<sup>67, 78, 79</sup> However, it is difficult to assign a precise contribution to catalysis from specific active site interactions, as perturbing features of the active site by mutagenesis often leads to disruption of multiple interactions and thus cannot be interpreted as evidence for the importance of a particular interaction.<sup>17</sup> The KIE approach circumvents this limitation of site-directed mutagenesis by introducing the smallest possible perturbation to a specific site in the substrate and provides information on both the nature of the transition state and interactions between the active site and the transition state. The data support previous models suggested from extensive structural and functional data that the active site Zn<sup>2+</sup> ions in AP form strong interactions with oxygen atoms of the phosphate ester in the transition state.<sup>7–9, 12, 43, 47, 80</sup> Nevertheless, challenges remain in quantitatively describing how the various active site interactions contribute to catalysis and understanding how these interactions work together to lead to the enormous rate enhancements achieved by enzymes.

## Supplementary Material

Refer to Web version on PubMed Central for supplementary material.

## Abbreviations

<b>AP</b>	alkaline phosphatase
<b>wt</b>	wild type
<b>LFER</b>	linear free energy relationship
<b>KIE</b>	kinetic isotope effect
<b>pNPP</b>	<i>p</i> -nitrophenyl phosphate
<b>mNBP</b>	<i>m</i> -nitrobenzyl phosphate
<b>pNPPS</b>	<i>p</i> -nitrophenyl phosphorothioate
<b>PTP</b>	protein tyrosine phosphatase
<b>G6P</b>	glucose 6-phosphate

## Acknowledgments

This work was supported by a grant to D.H. from the NIH (GM64798) and to A.H. from the NIH (GM47297). J.G.Z. was supported in part by a Hertz Foundation Graduate Fellowship. We thank members of the Hengge and Herschlag labs for comments on the manuscript, Helen Wiersma for providing additional purified alkaline phosphatase for kinetic measurements, and an anonymous reviewer for helpful comments and suggestions.

## References

1. Lad C, Williams NH, Wolfenden R. Proc. Natl. Acad. Sci. U.S.A. 2003; 100:5607–5610. [PubMed: 12721374]
2. Polanyi MZ. Elektrochem. Z. 1921; 27:142.
3. Pauling L. Chem. Eng. News. 1946; 24:1375–1377.
4. Wolfenden R. Acc. Chem. Res. 1972; 5:10–18.
5. Lienhard GE. Science. 1973; 180:149–154. [PubMed: 4632837]
6. Jencks, WP. Catalysis in Chemistry and Enzymology. New York: Dover Publications, Inc; 1987.
7. Kim EE, Wyckoff HW. J. Mol. Biol. 1991; 218:449–464. [PubMed: 2010919]
8. Holtz KM, Stec B, Kantrowitz ER. J. Biol. Chem. 1999; 274:8351–8354. [PubMed: 10085061]
9. Coleman JE. Annu. Rev. Biophys. Biomol. Struct. 1992; 21:441–483. [PubMed: 1525473]

10. O'Brien PJ, Herschlag D. *J. Am. Chem. Soc.* 1999; 121:11022–11023.
11. Hollfelder F, Herschlag D. *Biochemistry.* 1995; 34:12255–12264. [PubMed: 7547968]
12. O'Brien PJ, Herschlag D. *Biochemistry.* 2002; 41:3207–3225. [PubMed: 11863460]
13. Nikolic-Hughes I, Rees DC, Herschlag D. *J. Am. Chem. Soc.* 2004; 126:11814–11819. [PubMed: 15382915]
14. See references in Zalatan and Herschlag, 2006.<sup>44</sup>
15. See references in O'Brien and Herschlag, 1999, and Nikolic-Hughes, Rees, and Herschlag, 2004.<sup>10, 13</sup> See also: (a) Lahiri SD, Zhang GF, Dunaway-Mariano D, Allen KN. *Science.* 2003; 299:2607–2071. (b) Allen KN, Dunaway-Mariano D. *Trends Biochem Sci.* 2004; 29:495–503. [PubMed: 15337123] (c) Krishnamurthy H, Lou HF, Kimple A, Vieille C, Cukier RI. *Proteins.* 2005; 58:88–100. [PubMed: 15521058] (d) Bellinzoni M, Haouz A, Grana M, Munier-Lehmann H, Shepard W, Alzari PM. *Protein Sci.* 2006; 15:1489–1493. [PubMed: 16672241] (e) Hartmann MD, Bourenkov GP, Oberschall A, Strizhov N, Bartunik HD. *J. Mol. Biol.* 2006; 364:411–423. [PubMed: 17020768] (f) Wittinghofer A. *Trends Biochem. Sci.* 2006; 31:20–23. [PubMed: 16356724]. Note that the data reported in (a) has recently been reexamined in: (g) Baxter NJ, Olguin LF, Golicnik M, Feng G, Hounslow AM, Bermel W, Blackburn GM, Hollfelder F, Waltho JP, Williams NH. *Proc. Natl. Acad. Sci. U.S.A.* 2006; 103:14732–14737. [PubMed: 16990434]
16. Hengge AC. *Acc. Chem. Res.* 2002; 35:105–112. [PubMed: 11851388]
17. Kraut DA, Carroll KS, Herschlag D. *Annu. Rev. Biochem.* 2003; 72:517–571. [PubMed: 12704087]
18. Chaidaroglou A, Brezinski DJ, Middleton SA, Kantrowitz ER. *Biochemistry.* 1988; 27:8338–8343. [PubMed: 3072019]
19. Hengge AC, Edens WA, Elsing H. *J. Am. Chem. Soc.* 1994; 116:5045–5049.
20. Catrina IE, Hengge AC. *J. Am. Chem. Soc.* 2003; 125:7546–7552. [PubMed: 12812494]
21. Grzyska PK, Czyryca PG, Purcell J, Hengge AC. *J. Am. Chem. Soc.* 2003; 125:13106–13111. [PubMed: 14570483]
22. O'Brien PJ, Herschlag D. *Biochemistry.* 2001; 40:5691–5699. [PubMed: 11341834]
23. Gill SC, von Hippel PH. *Anal. Biochem.* 1989; 182:319–326. [PubMed: 2610349]
24. Lanzetta PA, Alvarez LJ, Reinach PS, Candia OA. *Anal. Biochem.* 1979; 100:95–97. [PubMed: 161695]
25. Bigeleisen J, Wolfsberg M. *Adv. Chem. Phys.* 1958; 1:15–76.
26. Caldwell SR, Raushel FM, Weiss PM, Cleland WW. *Biochemistry.* 1991; 30:7444–7450. [PubMed: 1649629]
27. Kirby AJ, Jencks WP. *J. Am. Chem. Soc.* 1965; 87:3209–3216.
28. Kirby AJ, Varvoglis AG. *J. Am. Chem. Soc.* 1967; 89:415–423.
29. Thatcher GRJ, Kluger R. *Adv. Phys. Org. Chem.* 1989; 25:99–265.
30. Hengge AC. *Adv. Phys. Org. Chem.* 2005; 40:49–108.
31. Cleland WW, Hengge AC. *Chem. Rev.* 2006; 106:3252–3278. [PubMed: 16895327]
32. Holtz KM, Catrina IE, Hengge AC, Kantrowitz ER. *Biochemistry.* 2000; 39:9451–9458. [PubMed: 10924140]
33. Footnote 2
34. Jencks, WP.; Regenstein, J. *Ionization Constants of Acids and Bases.* In: Fasman, GD., editor. *Handbook of Biochemistry and Molecular Biology.* Cleveland, OH: CRC; 1976.
35. Sowa GA, Hengge AC, Cleland WW. *J. Am. Chem. Soc.* 1997; 119:2319–2320.
36. Anderson MA, Shim H, Raushel FM, Cleland WW. *J. Am. Chem. Soc.* 2001; 123:9246–9253. [PubMed: 11562204]
37. Gerratana B, Sowa GA, Cleland WW. *J. Am. Chem. Soc.* 2000; 122:12615–12621.
38. Butcher WW, Westheimer FH. *J. Am. Chem. Soc.* 1955; 77:2420–2424.
39. Kumamoto J, Westheimer FH. *J. Am. Chem. Soc.* 1955; 77:2515–2518.
40. Bunton CA, Llewellyn DR, Oldham KG, Vernon CA. *J. Chem. Soc.* 1958:3574–3587.
41. Bunton CA, Fendler EJ, Humeres E, Yang KU. *J. Org. Chem.* 1967; 32:2806–2811.
42. Parente JE, Risley JM, Van Etten RL. *J. Am. Chem. Soc.* 1984; 106:8156–8161.

43. Nikolic-Hughes I, O'Brien PJ, Herschlag D. *J. Am. Chem. Soc.* 2005; 127:9314–9315. [PubMed: 15984827]
44. Zalatan JG, Herschlag D. *J. Am. Chem. Soc.* 2006; 128:1293–1303. [PubMed: 16433548]
45. Labow BI, Herschlag D, Jencks WP. *Biochemistry.* 1993; 32:8737–8741. [PubMed: 8395879]
46. Simopoulos TT, Jencks WP. *Biochemistry.* 1994; 33:10375–10380. [PubMed: 8068674]
47. Catrina I, O'Brien PJ, Purcell J, Nikolic-Hughes I, Zalatan JG, Hengge AC, Herschlag D. *J. Am. Chem. Soc.* 2007; 129:5760–5765. [PubMed: 17411045]
48. Weiss PM, Cleland WW. *J. Am. Chem. Soc.* 1989; 111:1928–1929.
49. Hengge AC, Hess RA. *J. Am. Chem. Soc.* 1994; 116:11256–11263.
50. Sawyer CB, Kirsch JF. *J. Am. Chem. Soc.* 1973; 95:7375–7381.
51. O'Leary MH, Marlier JF. *J. Am. Chem. Soc.* 1979; 101:3300–3306.
52. Blanchard JS, Cleland WW. *Biochemistry.* 1980; 19:4506–4513. [PubMed: 7407088]
53. Bahnson BJ, Anderson VE. *Biochemistry.* 1989; 28:4173–4181. [PubMed: 2765479]
54. Gorenstein DG, Lee YG, Kar D. *J. Am. Chem. Soc.* 1977; 99:2264–2267.
55. The value of  $^{18}(V/K)_{\text{nonbridge}}$  for wt AP-catalyzed hydrolysis of glucose 6-phosphate (G6P) has been reported to be 0.9994.<sup>48</sup> Based on the results reported herein, we would have expected a large inverse value of  $^{18}(V/K)_{\text{nonbridge}}$  for G6P hydrolysis similar to the values observed for pNPP<sup>2-</sup> and mNBP<sup>2-</sup>. However, it is possible that the chemical step is not rate-determining for AP-catalyzed G6P hydrolysis. The chemical step is rate-determining for simple alkyl phosphates with leaving group pK<sub>a</sub> values >14 (Figure 2),<sup>12</sup> but mNBP<sup>2-</sup> (leaving group pK<sub>a</sub> 14.9) reacts faster than expected, close to the limit at which a non-chemical step becomes rate determining (Figure 2). We have suggested above that the increased reactivity of mNBP<sup>2-</sup> is due to additional active site binding interactions with the large benzyl leaving group. G6P has a similarly large leaving group and may also benefit from active site interactions that lead to a faster-than-expected reaction rate that is limited by a non-chemical step. The pK<sub>a</sub> of glucose at the 6-OH position has not been measured, but it is likely to be lower than 16, the value for ethanol,<sup>34</sup> because the neighboring hydroxyl group can provide an intramolecular hydrogen bond.
56. Feder HM, Taube H. *J. Chem. Phys.* 1952; 20:1335–1336.
57. Taube H. *J. Phys. Chem.* 1954; 58:523–528.
58. Cassano AG, Anderson VE, Harris ME. *Biochemistry.* 2004; 43:10547–10559. [PubMed: 15301552]
59. Nelson BN, Exarhos GJ. *J. Chem. Phys.* 1979; 71:2739–2747.
60. Stangret J, Savoie R. *Can. J. Chem.* 1992; 70:2875–2883.
61. de la Fuente M, Hernanz A, Navarro R. *J. Biol. Inorg. Chem.* 2004; 9:973–986. [PubMed: 15452776]
62. Koleva VG. *Spectrochim. Acta A.* 2007; 66:413–418.
63. Jones JP, Weiss PM, Cleland WW. *Biochemistry.* 1991; 30:3634–3639. [PubMed: 2015221]
64. Hoff RH, Mertz P, Rusnak F, Hengge AC. *J. Am. Chem. Soc.* 1999; 121:6382–6390.
65. Hengge AC, Martin BL. *Biochemistry.* 1997; 36:10185–10191. [PubMed: 9254616]
66. Martin BL, Jurado LA, Hengge AC. *Biochemistry.* 1999; 38:3386–3392. [PubMed: 10079083]
67. Hengge, AC. Transfer of the PO<sub>3</sub><sup>2-</sup> group. In: Sinnott, ML., editor. *Comprehensive Biological Catalysis*. London: Academic Press; 1998. p. 517-542.
68. O'Brien PJ, Herschlag D. unpublished data.
69. Shannon RD. *Acta Crystallogr.* 1976; A32:751–767.
70. Brautigam CA, Steitz TA. *J. Mol. Biol.* 1998; 277:363–377. [PubMed: 9514742]
71. The catalytic proficiency is defined as the ratio of the second order rate constants for enzymatic and solution reactions ( $k_{\text{cat}}/K_M/k_W$ ). R166S AP has a catalytic proficiency of  $2 \times 10^{15}$  for pNPP<sup>2-</sup> hydrolysis<sup>43</sup> and  $>10^{23}$  for methyl phosphate hydrolysis.<sup>1, 10</sup> The overall difference in catalytic proficiency between pNPP<sup>2-</sup> and methyl phosphate is  $>10^8$ -fold.
72. Richard JP, Huber RE, Lin S, Heo C, Amyes TL. *Biochemistry.* 1996; 35:12377–12386. [PubMed: 8823173]
73. Thompson JE, Raines RT. *J. Am. Chem. Soc.* 1994; 116:5467–5468. [PubMed: 21391696]

74. Hondal RJ, Bruzik KS, Zhao Z, Tsai MD. *J. Am. Chem. Soc.* 1997; 119:5477–5478.
75. Hondal RJ, Zhao Z, Kravchuk AV, Liao H, Riddle SR, Yue X, Bruzik KS, Tsai MD. *Biochemistry.* 1998; 37:4568–4580. [PubMed: 9521777]
76. Ostanin K, Van Etten RL. *J. Biol. Chem.* 1993; 268:20778–20784. [PubMed: 8407904]
77. Whiteson KL, Chen Y, Chopra N, Raymond AC, Rice PA. *Chem. Biol.* 2007; 14:121–129. [PubMed: 17317566]
78. Knowles JR. *Ann. Rev. Biochem.* 1980; 49:877–919. [PubMed: 6250450]
79. Maegley KA, Admiraal SJ, Herschlag D. *Proc. Natl. Acad. Sci. U.S.A.* 1996; 93:8160–8166. [PubMed: 8710841]
80. Murphy JE, Stec B, Ma L, Kantrowitz ER. *Nat. Struct. Biol.* 1997; 4:618–622. [PubMed: 9253408]
81. Grzyska PK, Czyryca PG, Purcell J, Hengge AC. *J. Am. Chem. Soc.* 2007; 129:5298.
82. Czyryca PG, Hengge AC. *Biochim. Biophys. Acta.* 2001; 1547:245–253. [PubMed: 11410280]
83. Frey PA, Sammons RD. *Science.* 1985; 228:541–545. [PubMed: 2984773]

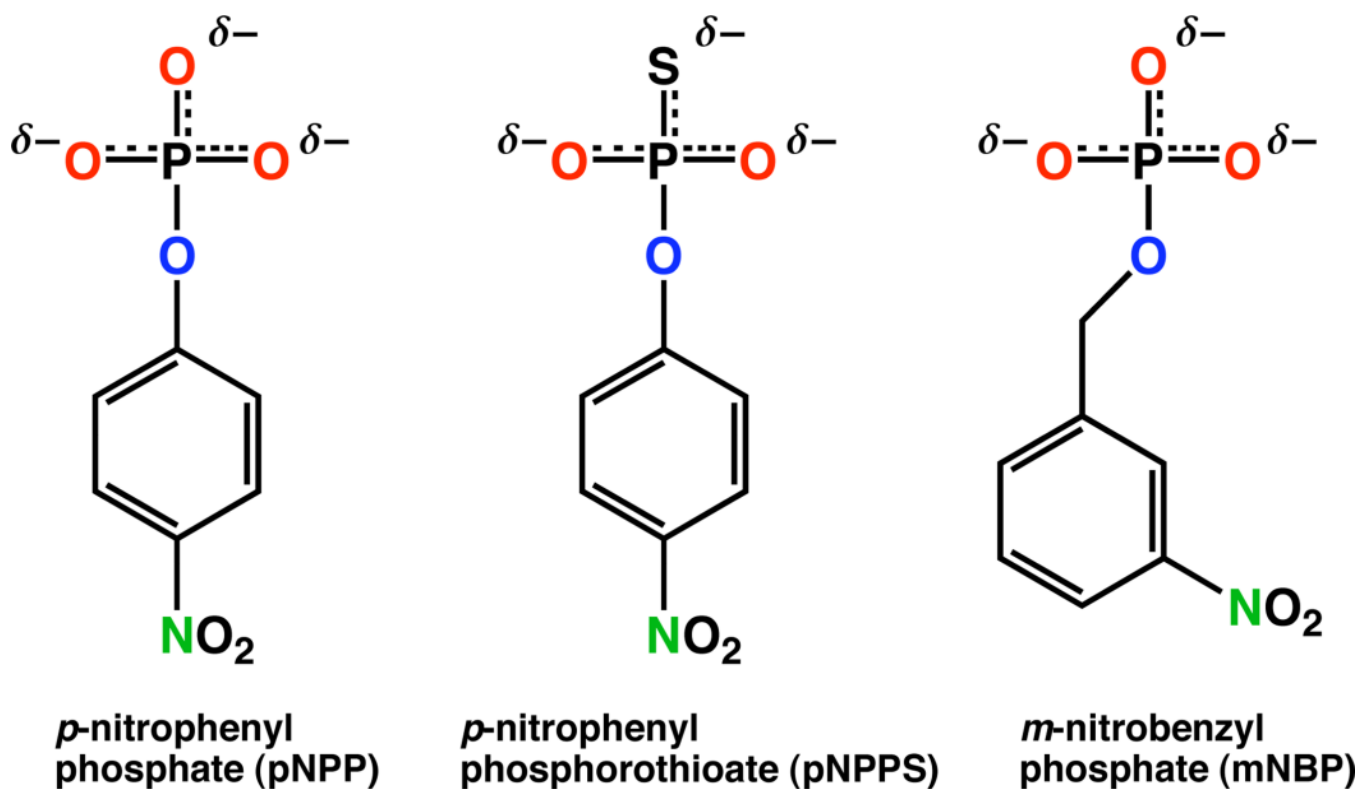


**Figure 1.**

Phosphate and phosphorothioate esters for which isotope effects are reported: red, nonbridge phosphoryl oxygen atoms [ $^{18}(V/K)_{\text{nonbridge}}$ ]; blue, bridge oxygen atom, site of bond fission [ $^{18}(V/K)_{\text{bridge}}$ ]; green, nitrogen atom of the leaving group [ $^{15}(V/K)$ ]. The structures are depicted with partial double bonds to emphasize that the nonbridging oxygen atoms that contribute to  $^{18}(V/K)_{\text{nonbridge}}$  are formally equivalent when the substrates are free in solution. For simplicity, the P-S and P-O bonds of pNPPS are depicted with the same partial double bond character, although it is likely that the P-S bond has more single bond character than the P-O bonds.<sup>43, 83</sup>



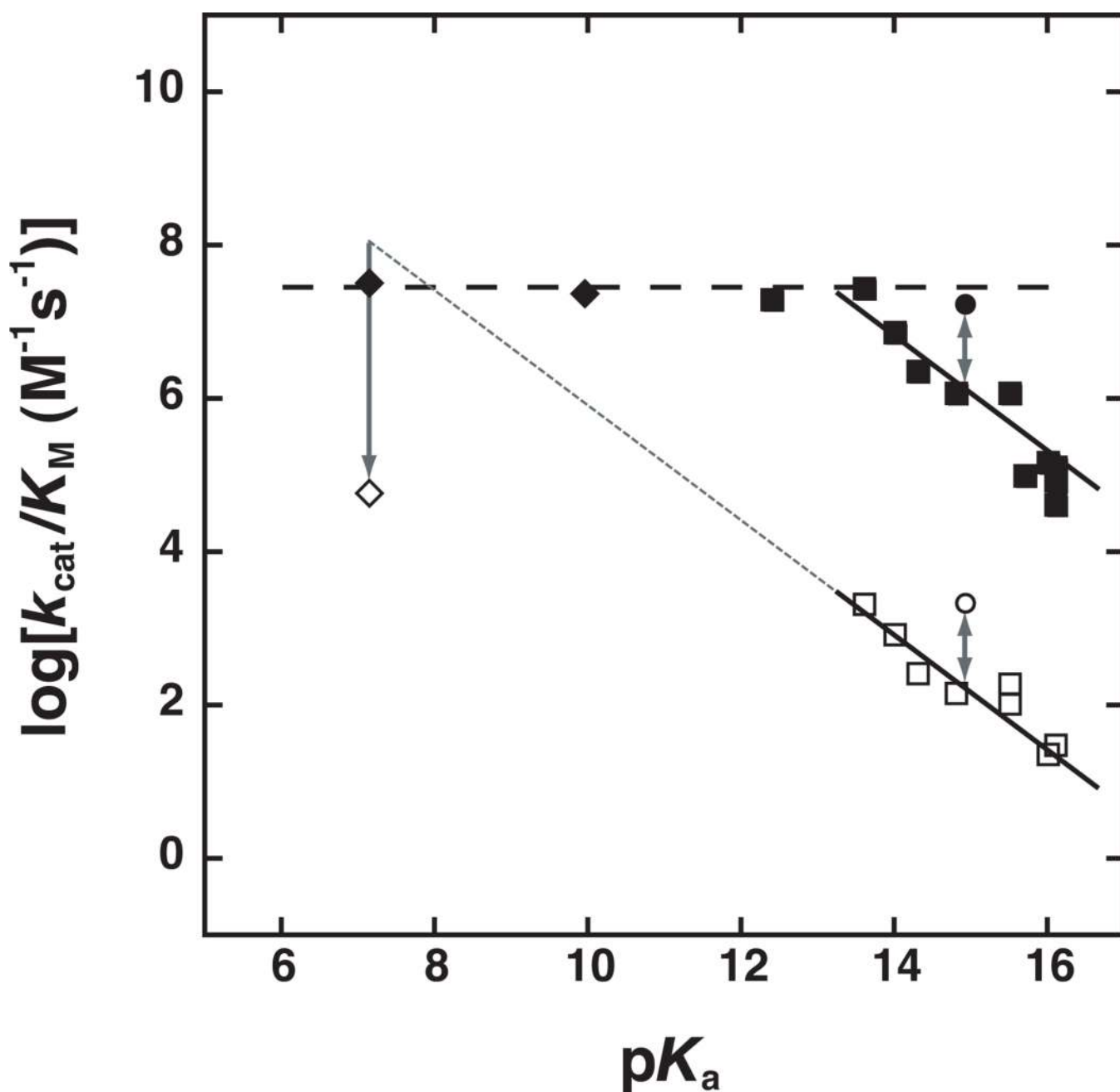


**Figure 2.**

Compilation of kinetic data for the reactions of wt and R166S AP, represented by closed and open symbols, respectively. Reactions of alkyl phosphates ( $\blacksquare$ ,  $\square$ ) give values of  $\beta_{lg}$  of  $-0.85 \pm 0.1$  and  $-0.66 \pm 0.1$  respectively for reactions with wt and R166S AP.<sup>10, 12</sup> Reactions of aryl phosphates ( $\blacklozenge$ ) with wt AP are limited by a non-chemical step (dashed line).<sup>12</sup> The rate constant for reaction of the aryl phosphate  $pNPP^{2-}$  ( $\diamond$ ) with R166S AP<sup>22</sup> deviates negatively from the value expected by extrapolation from the line for alkyl phosphates (dotted line and single-headed arrow). Rate constants for the reactions of  $mNBP^{2-}$  with wt and R166S AP ( $\bullet$ ,  $\circ$ ) deviate positively from the values expected from the line for alkyl phosphates (double-headed arrows).

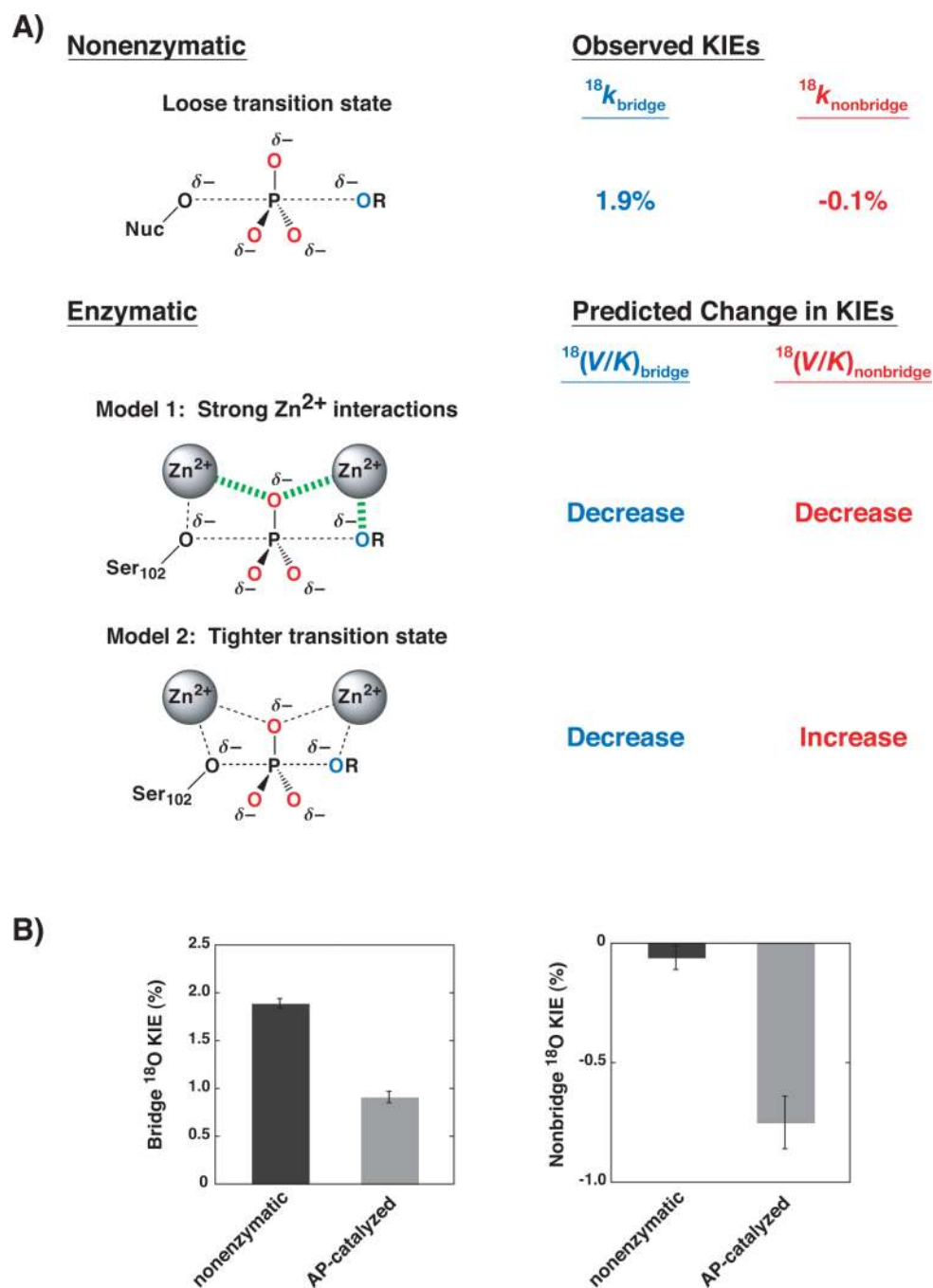
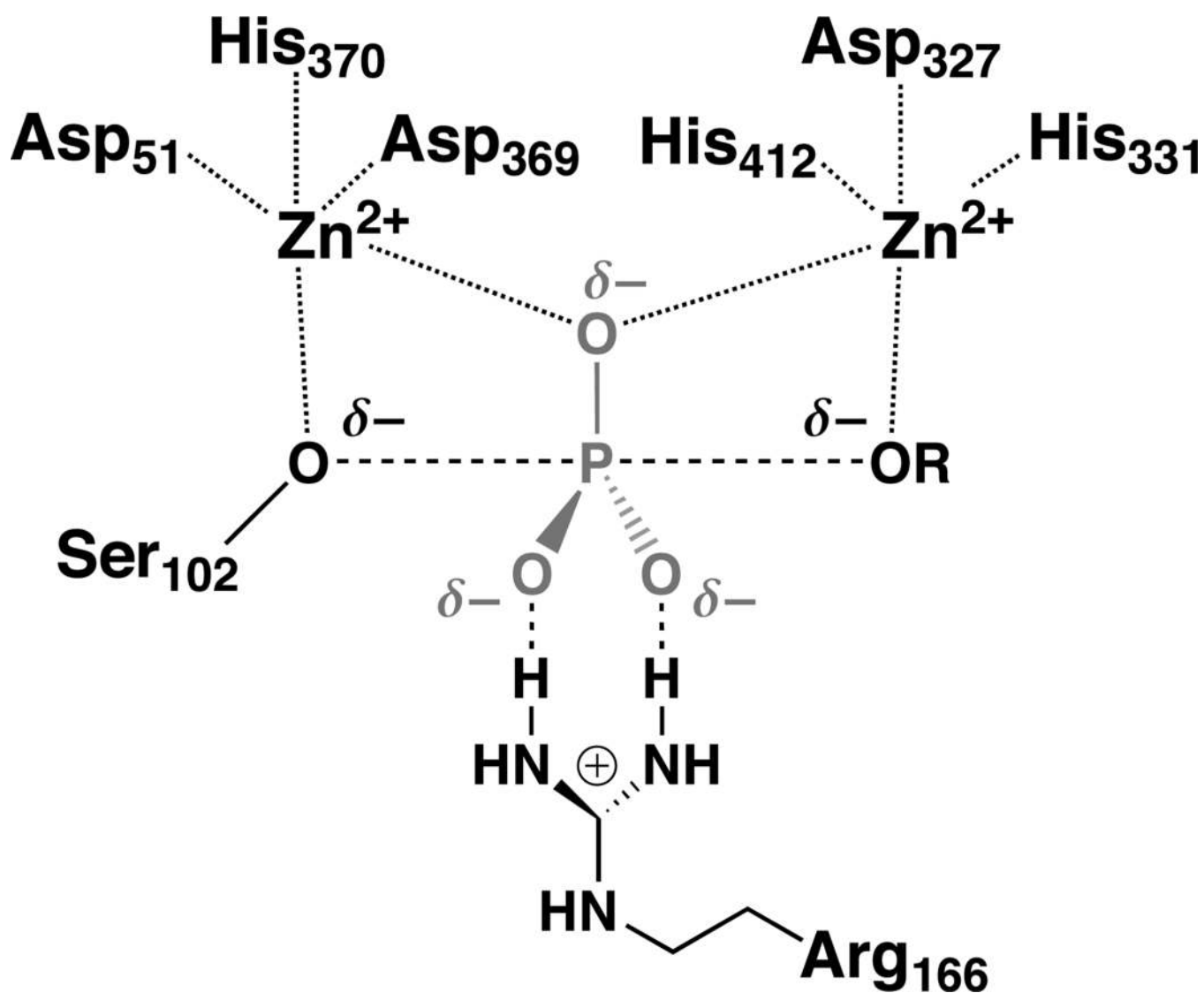
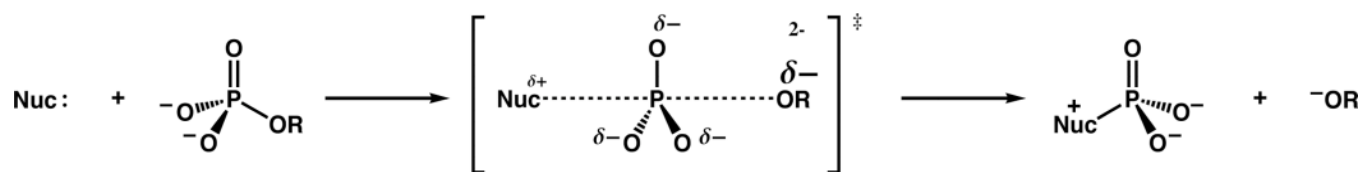


**Figure 3.** KIEs for AP-catalyzed reactions are different from the corresponding solution reaction. A) Predicted direction of changes in KIEs relative to the solution reaction for two different models for behavior of phosphate monoester substrates in the AP active site. In model 1, the transition state is loose, similar to that in solution, and strong interactions with active site metal ions lead to decreases in both  $^{18}(V/K)_{\text{bridge}}$  and  $^{18}(V/K)_{\text{nonbridge}}$ . In model 2, AP catalyzes phosphate monoester hydrolysis through a tighter transition state than that in solution. This model predicts a decrease in  $^{18}(V/K)_{\text{bridge}}$  and an increase in  $^{18}(V/K)_{\text{nonbridge}}$  based on comparisons to corresponding solution reactions.<sup>16</sup> B) The observed values of both  $^{18}(V/K)_{\text{bridge}}$  and  $^{18}(V/K)_{\text{nonbridge}}$  for AP-catalyzed pNPP<sup>2-</sup> hydrolysis decrease

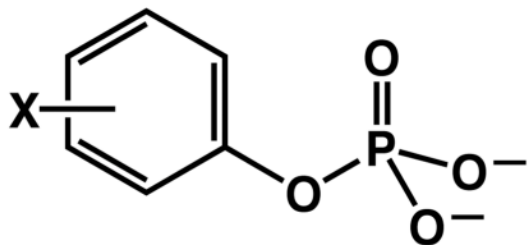
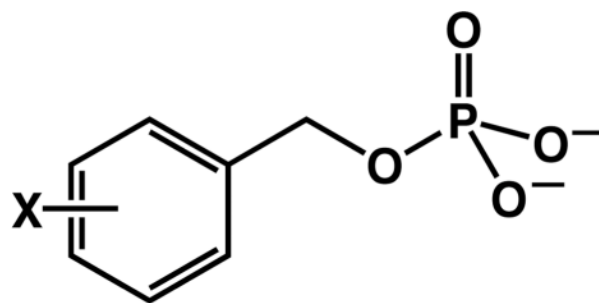
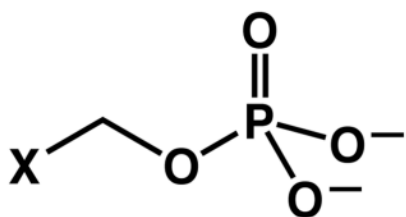
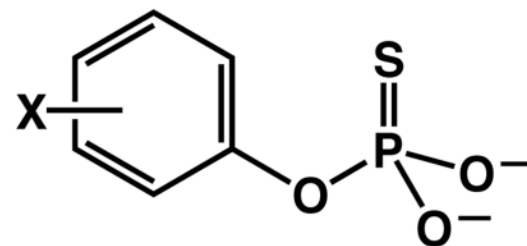
relative to the corresponding solution reaction, consistent with model 2. Isotope effects are expressed as a percentage difference from unity [ $KIE_{\%} = (KIE_{\text{obs}} - 1) * 100$ ]. Values for the nonenzymatic reaction are shown in black and values for the AP-catalyzed reaction are shown in grey.



**Scheme 1.**  
Transition state model for phosphoryl transfer catalyzed by AP based on the structure with a bound vanadate ligand.<sup>7, 8</sup>



**Scheme 2.**  
Phosphate monoester hydrolysis through a loose transition state.

**Aryl phosphates (◆)****Benzyl phosphates (●)****Alkyl phosphates (X ≠ Ph) (■)****Aryl phosphorothioates**

Scheme 3.

Table 1

Kinetic Isotope Effects<sup>a</sup>

Enzymatic Reactions <sup>b</sup>	Substrate	<sup>15</sup> (V/K)	<sup>18</sup> (V/K) <sub>bridge</sub>	<sup>18</sup> (V/K) <sub>nonbridge</sub>
wt AP <sup>19</sup>	pNPP <sup>2-</sup>	1.0003 (2)	1.0003 (4)	0.9982 (1)
wt AP	mNBP <sup>2-</sup>	0.9999 (4)	1.0072 (7)	0.9988 (4)
wt AP	pNPPS <sup>2-</sup>	1.0005 (2)	1.0094 (4)	0.9760 (22)
R166S AP <sup>47</sup>	pNPP <sup>2-</sup>	1.0007 (1)	1.0091 (6)	0.9925 (11)
R166S AP	mNBP <sup>2-</sup>	n.d. <sup>c</sup>	1.0199 (13)	0.9933 (4)
R166S AP	pNPPS <sup>2-</sup>	1.0006 (1)	1.0098 (3)	0.9768 (25)
Uncatalyzed Reactions	Substrate	<sup>15</sup> k	<sup>18</sup> k <sub>bridge</sub>	<sup>18</sup> k <sub>nonbridge</sub>
At 95 °C <sup>19</sup>	pNPP <sup>2-</sup>	1.0028 (2)	1.0189 (5)	0.9994 (5)
<i>Estimated</i> <sup>d</sup>	mNBP <sup>2-</sup>	1.0000	~1.04–1.06	~1.00
At 50 °C <sup>20</sup>	pNPPS <sup>2-</sup>	1.0027 (1)	1.0237 (7)	1.0135 (13)
At 95 °C <sup>19</sup>	pNPP <sup>1-</sup>	1.0004 (2)	1.0087 (3)	1.0184 (5)
At 115 °C <sup>21</sup>	mNBP <sup>1-</sup>	1.0000 (1)	1.0157 (9)	1.0151 (2)
At 30 °C <sup>20</sup>	pNPPS <sup>1-</sup>	1.0005 (1)	1.0091 (7)	1.0221 (4)

<sup>a</sup> Standard errors for the last decimal place(s) are in parenthesis. The nonbridge KIEs are the overall effects per molecule. The corresponding per atom isotope effects are the cube roots (in the case of phosphate esters) or the square roots (in the case of phosphorothioate esters) of the values reported above. Data for the reaction of wt and R166S AP with pNPP<sup>2-</sup> and for solution reactions are from previous work.<sup>19–21, 47</sup> Data for all other reactions were obtained for this work. The value of <sup>18</sup>k<sub>bridge</sub> of 1.0157 for mNBP<sup>1-</sup> has been corrected from the value originally reported in Grzyska et al., 2003.<sup>21, 81</sup>

<sup>b</sup> Enzymatic reactions with pNPP<sup>2-</sup> were conducted at 25 °C, and enzymatic reactions with mNBP<sup>2-</sup> were conducted at 30 °C. The reactions with pNPPS<sup>2-</sup> were conducted at 35 °C for wt AP and 25 °C for R166S AP. Although differences in temperature can effect the observed KIEs, these effects are small and do not affect the conclusions drawn herein.<sup>20, 82</sup>

<sup>c</sup> Not determined.

<sup>d</sup> KIEs for mNBP<sup>2-</sup> hydrolysis in solution cannot be measured because hydrolysis is dominated by alternative reaction pathways.<sup>1, 38–40</sup> The estimates shown were obtained as described in the main text.